

# Mechanistic Insight into the Synthesis of Higher Alcohols from Syngas: The Role of K Promotion on MoS<sub>2</sub> Catalysts

Vera P. Santos,<sup>†</sup> Bart van der Linden,<sup>†</sup> Adam Chojecki,<sup>‡</sup> Gerolamo Budroni,<sup>§</sup> Steven Corthals,<sup>§</sup> Hirokazu Shibata,<sup>‡</sup> Garry R. Meima,<sup>‡,§</sup> Freek Kapteijn,<sup>†</sup> Michiel Makkee,<sup>†</sup> and Jorge Gascon<sup>\*,†</sup>

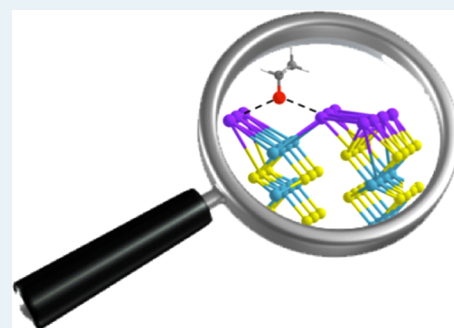
<sup>†</sup>Catalysis Engineering-Chemical Engineering Department, Delft University of Technology, Julianalaan 136, 2628 BL Delft, The Netherlands

<sup>‡</sup>Core R&D, <sup>§</sup>Hydrocarbons R&D, Dow Benelux B.V., P.O. Box 48, 4530 AA, Terneuzen, The Netherlands

## S Supporting Information

**ABSTRACT:** Operando infrared spectroscopy in combination with a kinetic study is used to elucidate the role of potassium on the conversion of carbon monoxide over K-promoted MoS<sub>2</sub> catalysts. More specifically, the initial break-in transient has been studied in detail. Stabilization of reaction intermediates, and effect of promoter on the intrinsic properties of MoS<sub>2</sub> are discussed. Adsorbed alkoxy species were found to play an important intermediate role in the syngas to alcohol route, and it was found that potassium stabilizes these species. Moreover, the electronic properties of MoS<sub>2</sub> change upon promotion, thereby allowing for a relatively easier activation of the CO molecule and a reduced hydrogenation activity toward alkanes.

**KEYWORDS:** biomass, syngas, higher alcohols, molybdenum disulfide, promoter potassium



In the last few decades, much attention has been paid to the synthesis of higher alcohols from coal or natural gas via syngas. Synthesis of higher alcohol is of interest because of the increasing price of petroleum, environmental concerns, and gasoline additive octane demands. Moreover, higher alcohols are preferred as gasoline boosters over the widely used methanol and ethanol because of their lower volatility, higher solubility in hydrocarbons, and higher calorific value.<sup>1</sup>

Coal, biomass, and natural gas can be converted via Fischer–Tropsch synthesis to higher alcohols over molybdenum, copper, iron, cobalt, or tungsten catalysts.<sup>2</sup> MoS<sub>2</sub> is one of the most promising catalytic systems, since it shows high resistance to sulfur poisoning and deactivation by coking.<sup>3</sup> In contrast to unpromoted MoS<sub>2</sub> that produces mainly hydrocarbons (C<sub>1</sub>–C<sub>6</sub>) at typical synthesis conditions ( $p > 30$  bar and  $T > 250$  °C), alkali-promoted MoS<sub>2</sub> display a high selectivity toward higher alcohols.<sup>3,4</sup>

Alkali promotion tunes kinetics and energetics of the adsorption of the reactants, hydrogen, and carbon monoxide, thereby affecting their relative surface coverage during reaction;<sup>5</sup> more specifically, alkali has been claimed to simultaneously be responsible for an increased nondissociative adsorption of CO and reduce the ability to activate hydrogen at the MoS<sub>2</sub> surface through site blocking on the sulfide surface.<sup>3</sup>

Moreover, some authors also suggest that the addition of potassium stabilizes oxygenate species, directing the synthesis toward alcohols rather than hydrocarbons.<sup>6</sup> However, hardly any experimental evidence has been presented to support these claims under industrially relevant reaction conditions.<sup>3</sup>

Here, we studied the role of alkali promotion on CO activation, stabilization of intermediates, and intrinsic properties of MoS<sub>2</sub> by combining operando spectroscopy and high-throughput (HT) kinetic experiments. Although several in-situ studies have been reported on alkali-promoted supported MoS<sub>2</sub> catalysts for the synthesis of higher alcohols,<sup>7</sup> only a few articles deal with infrared spectroscopy studies on bulk molybdenum sulfides.<sup>4a,b</sup> Surprisingly, in these studies, KBr was used as diluent, something striking when the role of potassium is to be unravelled.

In this work, we studied a series of bulk MoS<sub>2</sub> catalysts synthesized by thermal decomposition of ammonium tetrathiomolybdate. Alkali promotion was performed by physically mixing K<sub>2</sub>CO<sub>3</sub> with MoS<sub>2</sub> (see the Supporting Information for a detailed catalyst preparation).

The conversion profile and alcohol selectivity as a function of time-on-stream (TOS) for all catalysts are shown in Figure 1a. As expected, the presence of potassium on MoS<sub>2</sub> shifts the selectivity toward alcohols (C<sub>1</sub>–C<sub>4</sub> alcohols, 45% selectivity) and decreases the break-in period of MoS<sub>2</sub> (see the inset of Figure 1a). Selectivity to alcohols on K-MoS<sub>2</sub> increases monotonically with time on-stream. This transient period was associated with the spreading of the alkali promoter on the surface of MoS<sub>2</sub>.<sup>3,4,6c,8</sup> The promoter effect is also reflected in the observed apparent activation energy, which decreases from

Received: May 13, 2013

Revised: June 9, 2013

Published: June 18, 2013

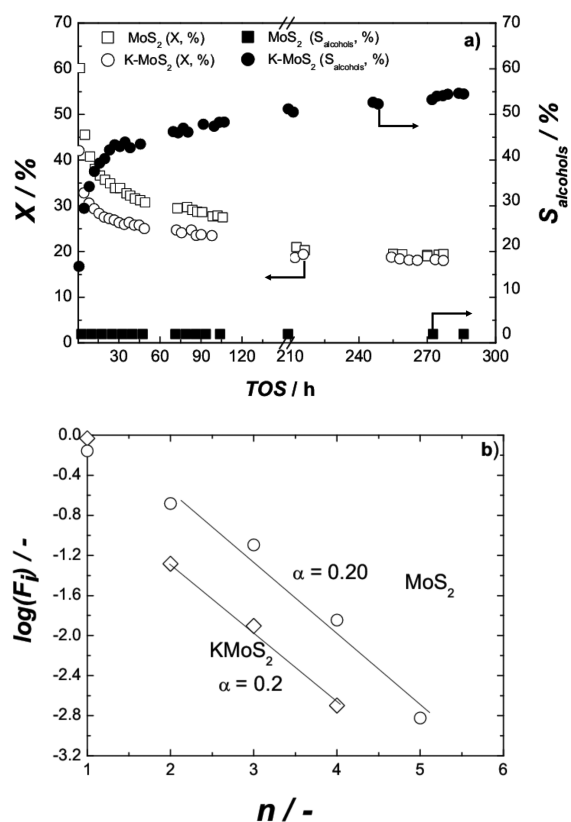


**Figure 1.** (a) Conversion ( $X$ , open symbols) and alcohol selectivity ( $S_{\text{alcohols}}$ , solid symbols) profiles; (b) ASF distribution plot of hydrocarbons and corresponding  $\alpha$  values for MoS<sub>2</sub> and K-MoS<sub>2</sub>. Catalytic tests were performed at 310 °C, 90 bar, and space velocity of 10 000 h<sup>-1</sup>. Selectivity to alcohols was calculated from the individual selectivities of methanol, ethanol,  $n$ -propanol, and  $n$ -butanol.

133 ± 2 to 60 ± 2 kJ/mol upon K promotion (see the Supporting Information). However, the chain growth probability for hydrocarbons,  $\alpha$ , remains constant, as depicted by the unchanged slope in the Anderson–Schultz–Flory (ASF) plots (Figure 1b).

The effect of potassium on the stabilization of surface intermediates and mechanism of alcohol formation was investigated by operando infrared spectroscopy (30 bar, 350 °C and a bed volume space velocity of 7000 h<sup>-1</sup>). To validate the operando DRIFTS at lower pressures, additional kinetic experiments were carried out at 30 bar, 350 °C and a bed volume space velocity of 4000 h<sup>-1</sup>. An excellent match between the high throughput (HT) experiments and operando DRIFTS was observed, and the same conversion level was achieved in both experimental setups ( $X \approx 2$ –4%). The conditioning of molybdenum sulfide catalysts is characterized by long transient periods (“break-in”; Figure 1a), accompanied by a continuous decrease in activity due to the permanent reconstruction of the active phase. However, the major significant differences in the evolution of the conversion of carbon monoxide and in product distribution occur during the first 24 h. For this reason, the DRIFT operando study was focused on this break-in period. The time-resolved DRIFTS spectra recorded during reductive polymerization of CO on K-MoS<sub>2</sub> are shown in Figure 2a.

The formation of hydrocarbons (mainly CH<sub>4</sub>) and CO<sub>2</sub> (gas phase) already from the very beginning of the break-in period is evidenced by the appearance of bands at 3014 and 2360 cm<sup>-1</sup>, respectively.

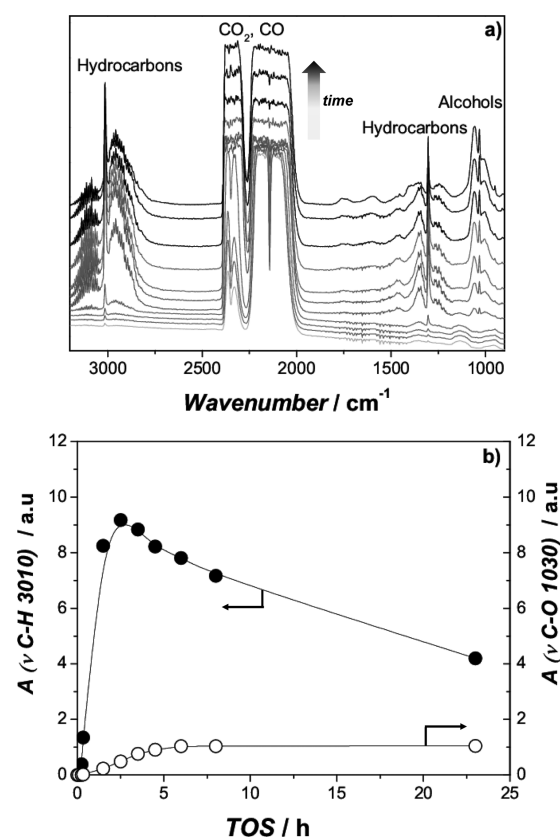


**Figure 2.** (a) In situ DRIFTS spectra of K-MoS<sub>2</sub> during catalytic hydrogenation of CO at 350 °C, 30 bar, CO/H<sub>2</sub>: 1, and space velocity of 7000 h<sup>-1</sup>. (b) Evolution of absorbance of hydrocarbons (@ 3010 cm<sup>-1</sup>) and alcohols (@ 1030 cm<sup>-1</sup>) as a function of TOS.

After ~3 h of reaction (induction period), another contribution at 1030 cm<sup>-1</sup> appears that is associated with the formation of alcohols (methanol and ethanol). At longer reaction times, bands between 1700 and 1500 cm<sup>-1</sup> (ν COO) also suggest the formation of other oxygenates, such as esters. The evolution of hydrocarbons and alcohols as a function of time-on-stream is shown in Figure 2b. A qualitative reproduction of the break-in profiles obtained from the HTs studies is obtained during the in situ DRIFTS experiments. The time-resolved DRIFTS spectra for the unpromoted system is summarized in Supporting Information Figure S2.

To elucidate the role of the alkali dispersion on the induction period, a second promoted sample was prepared by incipient wetness impregnation instead of physical mixing (Supporting Information Figure S3). Using this preparation approach, alcohols were already produced in the first minutes of reaction: clearly, the induction period is related to the potassium migration/redistribution and can be significantly shortened. This preparation approach was also used to test the promoter effect of precursors considered in the literature as “not selective” to alcohols, such as K<sub>2</sub>SO<sub>4</sub>.<sup>4c</sup>

In this case, the differences in selectivity are even more evident (Supporting Information Figure S3b): catalysts prepared by physical mixing do not produce alcohols, in agreement with literature,<sup>4c</sup> but in the case of incipient wetness impregnation, alcohols were formed after 30 min of reaction. Although the degree of promotion is lower than that for K<sub>2</sub>CO<sub>3</sub>, these findings demonstrate that the nature of the

promotional effects depends not only on the precursor,<sup>4c,6c,9</sup> but also on the way the alkali is incorporated.

The infrared spectrum of adsorbed species (after flushing the system with He) on promoted and unpromoted MoS<sub>2</sub> after 24 h TOS is presented in Figure 3. In the case of the unpromoted

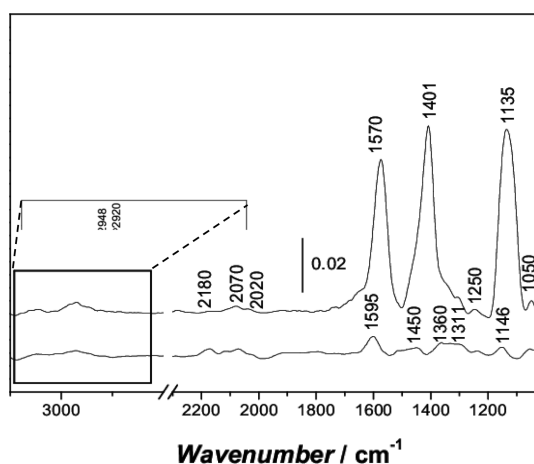


**Figure 3.** DRIFTS spectra of MoS<sub>2</sub> (down) and KMoS<sub>2</sub> (up) after 24 h of reaction, followed by flushing with helium at 350 °C and 1 bar (inset represents the C–H stretching region).

sample, the spectrum shows absorption bands in the region of 3120–2860 ( $\nu$  C–H), 2180–2020 ( $\nu$  C–O), 1600–1300 ( $\nu$  COO), and 1250–1146 cm<sup>-1</sup> ( $\nu$  S–O), assigned to the presence of adsorbed hydrocarbons, CO, oxygenates and oxidized sulfide species, respectively. The vibrational bands at 2920 ( $\nu_{\text{comb}}$ ), 2860 ( $\nu$  C–H), 1590 ( $\nu_a$  COO), and 1360–1311 ( $\nu_s$  COO)<sup>7a,10</sup> show that formates are the main oxygenates on the surface of MoS<sub>2</sub>. The intensity of these bands is low as a result of deposition of carbon (e.g. oligomerization, Boudouard reaction), as demonstrated by Raman spectroscopy (see the Supporting Information).

In the case of the promoted sample (K-MoS<sub>2</sub>), formate species (1570 ( $\nu_{\text{as}}$  COO), 1401 ( $\nu_s$  COO)), were also found, but the observed frequencies are shifted downward ( $\approx 20$  cm<sup>-1</sup>), which can be due to a different coordination with Mo surface or interaction with potassium cations. Moreover, in addition to formates, alkoxy species are also observed on the surface of the promoted sample (2950–2930 ( $\nu_a$  CH<sub>3</sub>), 2860 ( $\nu_s$  CH<sub>3</sub>), 1135 ( $\rho$  C–H), and 1050 ( $\nu$  C–O) cm<sup>-1</sup>).<sup>11</sup> The measured vibrational frequencies suggest that there is an electrostatic interaction between potassium and alkoxy species, forming stabilized complexes. These complexes can also explain the formation of methyl formates on K-MoS<sub>2</sub>,<sup>6a</sup>

The effect of potassium on the adsorption properties of MoS<sub>2</sub> was evaluated by infrared spectroscopy using CO as a probe molecule.

Electron probe microscopy analysis performed on the promoted catalyst showed that the distribution of K on the fresh K-MoS<sub>2</sub> catalyst is inhomogeneous and that a redispersion of K occurs upon exposure to reaction conditions (Supporting Information Figure S3). Because of the redispersion of K during the first reaction hours and the observed induction period for the production of alcohols, CO adsorption studies under IR were carried out after exposing K-MoS<sub>2</sub> to syngas for 3 h, at 350 °C and 30 bar. For comparison, the unpromoted sample underwent the same treatment. The  $\nu$  (CO) stretching

region of adsorbed carbon monoxide on these samples is shown in Figure 4.

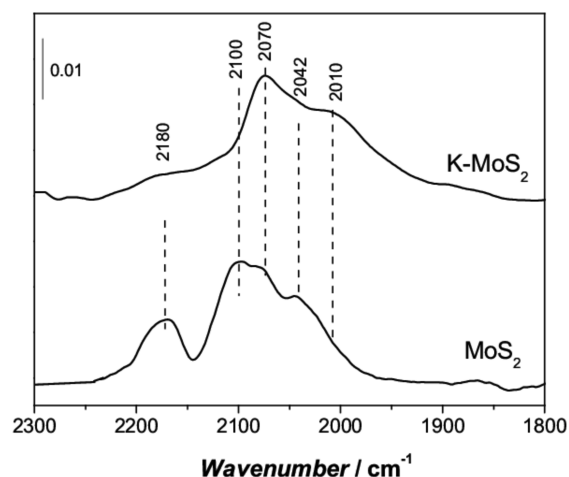


**Figure 4.** DRIFT spectra of adsorbed CO at room temperature on samples after syngas conversion at 350 °C and 30 bar for 3 h.

CO interaction with MoS<sub>2</sub> after syngas conditions at 350 °C gives rise to absorption bands at 2180, 2100, 2070, and 2042 cm<sup>-1</sup>. The first band corresponds to the fundamental C–O stretching mode of CO perturbed by the electrostatic field created by cations in Mo<sup>4+</sup> ← CO species. The bands at 2100, 2070, and 2042 cm<sup>-1</sup> correspond to the end-on adsorption of CO on coordinatively unsaturated sites (cus) of Mo<sup>δ+</sup> ( $\delta \approx 2$ ) having different local environments (edges and corners, respectively).<sup>12</sup> These reduced sites are created upon removal of sulfur at the edge and corner positions, exposing cus of Mo<sup>δ+</sup>. The presence of potassium significantly increases the back-donation of Mo, as observed by the shift of the absorption bands to lower wavenumbers. Moreover, the relative amount of edge sites decreased (band at 2100 cm<sup>-1</sup>), increasing that of corner sites, suggesting that potassium occupies many of these sites, decreasing the hydrogenation ability of promoted MoS<sub>2</sub>. In addition, the decrease in the absorption band at 2180 cm<sup>-1</sup> is indicative of a lower intrinsic Lewis acidity of MoS<sub>2</sub>.

In view of these results, we can rationalize the promotional effect of K as a charge transfer to the catalyst surface due to the low ionization potential of the alkali metal, decreasing both the work function of MoS<sub>2</sub> surface and its hydrogenation ability.<sup>5a,13</sup> In this way, the nondissociative adsorption of CO is favored against the hydrogen-assisted adsorption path (via formyl species, CHO), that readily would result in the formation of carbon and CH<sub>x</sub> species on the sulfide surface.<sup>5</sup>

According to obtained spectroscopic and kinetic data and the literature, the activation of CO over unpromoted MoS<sub>2</sub> proceeds via a hydrogen-assisted process through formyl intermediates (Supporting Information Figure S6).<sup>3,14</sup> These formyl (HC=O) species are mainly converted into CH<sub>x</sub> and carbon deposits at the surface of MoS<sub>2</sub>. The high hydrogenation activity of this catalyst leads mainly to hydrocarbons.<sup>6b,15</sup>

As observed by FT-IR, potassium promotion results in the formation of new active sites for activation of CO and drives the hydrogenation toward partially hydrogenated intermediates (alkoxy). We speculate that methoxides stabilized at the surface can either desorb in the form of methanol or react further with CO, giving methyl formates.<sup>6a</sup> In a similar fashion, the presence

of potassium in close vicinity to an adsorbed methyl group will favor CO insertion, stabilizing acyl intermediates<sup>6c</sup> that are further hydrogenated to ethoxy and, finally, to ethanol.<sup>6a</sup>

For the formation of higher alcohols (C<sub>3</sub>, C<sub>4</sub>) on the promoted catalysts, two different pathways would be feasible: (i) CO insertion<sup>6a</sup> and (ii) direct aldol condensation mechanism to a minor extent (Supporting Information Figure S7).<sup>3,6a,16</sup> To check to what extent aldol condensation plays an important role in the production of higher alcohols, additional kinetic experiments were performed with cofeeding syngas and ethanol. In the case of MoS<sub>2</sub>, the product stream contained only hydrocarbons (mainly ethane). As expected the conversion of alcohols to hydrocarbons takes place when no alkali is present. In contrast, in the case of K-MoS<sub>2</sub>, the addition of ethanol to the syngas feed boosted the production of higher alcohols, predominantly 1-propanol (dehydroxylation on Mo sites, followed by CO insertion) and 1-butanol (Supporting Information Figure S8). Furthermore, to reveal whether 1-butanol results from the self-coupling of ethanol or from consecutive CO addition reactions, we performed experiments cofeeding only ethanol and nitrogen. 1-Butanol was, indeed, obtained, along with ethyl acetate formed via ethanol dehydrogenation (the main product in the absence of hydrogen).<sup>17</sup>

From these experiments, we conclude that formation of higher alcohols proceeds not only via CO insertion, but also via aldol condensation of shorter alcohols.<sup>18</sup> Altogether, our results emphasize the complexity behind the synthesis of high alcohols from syngas and the delicate interplay between hydrocarbon and alcohol formation. For example, the formation of butanol may proceed via (i) formation of a propyl species on the surface of the catalyst, migration to a K site, and CO insertion with stabilization of the corresponding butoxide or (ii) via aldol condensation of ethanol with its corresponding aldehyde.

Summarizing, by combining a kinetic investigation and operando spectroscopy, the role of K as a promoter in MoS<sub>2</sub> catalysts was enlightened. The presence of K not only changes the electronic properties of the catalyst, but also stabilizes alkoxy species, contributing to the formation of higher alcohols via CO insertion and to a small extent by basic catalyzed aldol condensation. Moreover, the promotional effect depends strongly on the way the alkali is incorporated.

These insights can contribute to further improvements in the development of selective catalysts for the synthesis of higher alcohols from syngas.

## ■ ASSOCIATED CONTENT

### 📄 Supporting Information

Experimental details and additional figures. This material is available free of charge via the Internet at <http://pubs.acs.org>.

## ■ AUTHOR INFORMATION

### Corresponding Author

\*E-mail: [j.gascon@tudelft.nl](mailto:j.gascon@tudelft.nl).

### Notes

The authors declare no competing financial interest.

## ■ REFERENCES

- (1) Herman, R. G. *Catal. Today* **2000**, *55*, 233–245.
- (2) Herman, R. G. *Stud. Surf. Sci. Catal.* **1991**, *64*, 265.
- (3) Zaman, S.; Smith, K. J. *Catal. Rev.* **2012**, *54*, 41–132.
- (4) (a) Woo, H. C.; Park, K. Y.; Kim, Y. G. I.; Namau, S.; Lee, J. S. *Appl. Catal.* **1991**, *75*, 267–280. (b) Woo, H. C.; Nam, I. S.; Lee, J. S.;

Chung, J. S.; Lee, K. H.; Kim, Y. G. *J. Catal.* **1992**, *138*, 525–535. (c) Lee, J. S.; Kim, S. K.; Lee, H.; Nam, I. S.; Chung, J. S.; Kim, Y. G.; Woo, H. C. *Appl. Catal., A* **1994**, *110*, 11–25. (d) Murchison, D. A. M. C. B. U.S. Patent 4,151,190A 1979.

(5) (a) Ponec, V. *Stud. Surf. Sci. Catal.* **1991**, *64*, 117. (b) Sachtler, W. M. H.; Shriver, D. F.; Hollenberg, W. B.; Lang, A. F. *J. Catal.* **1985**, *92*, 429–431.

(6) (a) Santiesteban, J. G.; Bogdan, C. E.; Herman, R. G.; Klier, K. In *Proceedings 9th International Congress on Catalysis: Catalysis, Theory to Practice*; 1988, Vol. 2 C1 chemistry, pp 561. (b) Anderson, A. B.; Yu, J. *J. Catal.* **1989**, *119*, 135–145. (c) Woo, H. C.; Nam, I. S.; Lee, J. S.; Chung, J. S.; Kim, Y. G. *J. Catal.* **1993**, *142*, 672–690.

(7) (a) Tsyganenko, A. A.; Can, F.; Travert, A.; Maugé, F. *Appl. Catal., A* **2004**, *268*, 189–197. (b) Surisetty, V. R.; Dalai, A. K.; Kozinski, J. *Appl. Catal., A* **2010**, *385*, 153–162. (c) Surisetty, V. R.; Eswaramoorthi, I.; Dalai, A. K. *Fuel* **2012**, *96*, 77–84. (d) Koizumi, N.; Bian, G.; Murai, K.; Ozaki, T.; Yamada, M. *J. Mol. Catal. A: Chem.* **2004**, *207*, 173–182.

(8) Xiao, H.; Li, D.; Li, W.; Sun, Y. *Fuel Process. Technol.* **2010**, *91*, 383–387.

(9) Ferrari, D.; Budroni, G.; Bisson, L.; Rane, N. J.; Dickie, B. D.; Kang, J. H.; Rozeveld, S. J. *Appl. Catal., A* **2013**, DOI: 10.1016/j.apcata.2013.05.006.

(10) (a) Amenomiya, Y. *J. Catal.* **1979**, *57*, 64–71. (b) Fisher, I. A.; Bell, A. T. *J. Catal.* **1997**, *172*, 222–237. (c) Gopal, P. G.; Schneider, R. L.; Watters, K. L. *J. Catal.* **1987**, *105*, 366–372. (d) Huuhtanen, M.; Kolli, T.; Maunula, T.; Keiski, R. L. *Catal. Today* **2002**, *75*, 379–384. (e) Vayssilov, G. N.; Mihaylov, M.; Petkov, P. S.; Hadjiivanov, K. I.; Neyman, K. M. *Phys. Chem. C* **2011**, *115*, 23435–23454.

(11) Uvdal, P.; Weldon, M. K.; Friend, C. M. *Phys. Rev. B* **1994**, *50*, 12258–12261.

(12) (a) Travert, A.; Dujardin, C.; Maugé, F.; Cristol, S.; Paul, J. F.; Payen, E.; Bougeard, D. *Catal. Today* **2001**, *70*, 255–269. (b) Maugé, F.; Lavalley, J. C. *J. Catal.* **1992**, *137*, 69–76. (c) Pavão, A. C.; Guimarães, T. C. F.; Lie, S. K.; Taft, C. A.; Lester, W. A., Jr. *Theochem: J. Mol. Struct.* **1998**, *458*, 99–121. (d) Peri, J. B. *J. Phys. Chem.* **1982**, *86*, 1615–1622. (e) Zeng, T.; Wen, X. D.; Wu, G. S.; Li, Y. W.; Jiao, H. *Phys. Chem. B* **2005**, *109*, 2846–2854.

(13) Papageorgopoulos, C. A.; Kamaratos, M.; Kennou, S.; Vlachos, D. *Stud. Surf. Sci. Catal.* **1991**, *251–252*, 1057–1061.

(14) Nehasil, V.; Stará, I.; Matolín, V. *Stud. Surf. Sci. Catal.* **1995**, *331–333* (Part A), 105–109.

(15) Huang, M.; Cho, K. *J. Phys. Chem. C* **2009**, *113*, 5238–5243.

(16) Xu, X. D.; Doesburg, E. B. M.; Scholten, J. J. F. *Catal. Today* **1987**, *2*, 125–170.

(17) Santacesaria, E.; Carotenuto, G.; Tesser, R.; Serio, M. D. *Chem. Eng. J.* **2012**, *179*, 209–220.

(18) (a) Christensen, J. M.; Jensen, P. A.; Schiødt, N. C.; Jensen, A. D. *ChemCatChem* **2010**, *2*, 523–526. (b) Bian, G.-z.; Fan, L.; Fu, Y.-l.; Fujimoto, K. *Ind. Eng. Chem. Res.* **1998**, *37*, 1736–1743.